Eur Biophys J (1994) 23:253–262

European Biophysics Journal

Contributions of tryptophan side chains to the far-ultraviolet circular dichroism of proteins

Robert W. Woody

Department of Biochemistry and Molecular Biology, Colorado State University, Fort Collins, CO 80523, USA

Received: 10 March 1994 / Accepted: 29 April 1994

Abstract. It has often been assumed that the role of aromatic side chains in the far-ultraviolet region of protein circular dichroism (CD) is negligible. However, some proteins have positive CD bands in the 220–230 nm region which are almost certainly due to aromatic side chains. The contributions to the CD of interactions between tryptophan side chains and the nearest neighbor peptide groups have been studied, focusing on the indole B_b transition which occurs near 220 nm. Calculations on idealized peptide conformations show that the CD depends strongly on both backbone and side-chain conformation. Because of the low symmetry of indole, rotation about the $C_\beta C_\gamma$ bond (dihedral angle χ_2) by 180° generally leads to large changes in the CD, often causing the B_b band to reverse sign. When side-chain conformational preferences are taken into account, there is no strong bias for either positive or negative B_b rotational strengths. The observation that simple tryptophan derivatives such as N-acetyl-L-tryptophan methylamide have positive CD near 220 nm implies either that these derivatives prefer the α_R region over the β region, or that there is little preference for $\chi_2 < 180°$ over $\chi_2 > 180°$. Nearest-neighbor-only calculations on individual tryptophans in 15 globular proteins also reveal a small bias toward positive B_b bands. Rotational strengths of the B_b transition for some conformations can be as large as ~1.0 Debye-Bohr magnetons in magnitude, corresponding to maximum molar ellipticities greater than 10^5 deg cm^2/dmol. Although a substantial amount of cancellation occurs in most of the examples considered here, such CD contributions could be significant, especially in proteins of low helix content.

Key words: Tryptophan – Circular dichroism – Proteins – Side-chain conformation – Theory

Introduction

In many schemes for the analysis of protein secondary structure by CD, it is assumed that the contributions of side-chain chromophores to the far-ultraviolet CD are negligible. Among the standard amino acids, only those with aromatic functionalities (phenylalanine, tyrosine, tryptophan and histidine) are likely to make significant contributions. Aromatic chromophores have intense, fully allowed $\pi\pi^*$ transitions in the wavelength range (ca. 180–230 nm) commonly used for secondary structure analysis. In addition, the chromophore is attached to the β carbon in these amino acids, which brings it into relatively close proximity to the peptide backbone. Other side-chain chromophores have substantially weaker absorption bands in this region, and (except for cysteine, aspartate and asparagine) the chromophores are more distant from the backbone by one or more carbons.

Sears and Beychok (1973) reviewed the far-ultraviolet CD contributions of aromatic side chains in model compounds, noting that the N-acetyl aromatic amino acid amides (Shiraki 1969) all have positive bands near 220 nm. They suggested that, as a rule-of-thumb, a value of ~12 000 deg cm^2/dmol at 222 nm can be expected for each aromatic amino acid. Sears and Beychok also inferred from data on synthetic polypeptides and proteins that the aromatic side chains could make much larger contributions in the 200 nm region, of the order of 80 000 deg cm^2/dmol.

Woody (1978) reported calculations of the rotational strengths of the L_a (Platt 1949) bands of phenylalanine and tyrosine arising from interactions with the immediately neighboring amide chromophores. Theory predicted that these bands, giving rise to CD bands near 220 nm, although potentially being of either sign, have a strong tendency to be positive for the L-amino acid when the most favorable combination of backbone and side-chain conformation are considered. The calculations also gave rotational strengths for some specific conformations which were compatible with the large values inferred by Sears and Beychok (1973).

No comparable theoretical calculations have been reported on the far-ultraviolet CD of tryptophan-containing peptides, especially on the B_b (Platt 1949) transition of the indole group. In the present paper, I describe calculations on the contributions of tryptophan side chains to the CD of dipeptide fragments and globular proteins and discuss their implications for interpreting the far-ultraviolet CD of peptides and proteins.

The indole chromophore

The indole chromophore of tryptophan exhibits four readily identifiable electronic transitions in the wavelength region from 180–300 nm, as exemplified by the data given in Table 1 for 3-indolylacetic acid in water (Yamamoto and Tanaka 1972). This observation fits the theoretical picture developed by Platt (1949) for aromatic chromophores. In Platt's model, indole is considered as a perturbed cyclodecapentaene, a system with 10 π electrons. The covalent link between $C_{\delta 2}$ and $C_{\varepsilon 2}$ (IUPAC-IUB 1976) of the indole ring and the substitution of a nitrogen for two carbons constitute the perturbations. Such a system is predicted to have two low-energy excited states, L_b and L_a, and two high-energy excited states, B_b and B_a. Transitions from the ground state to the L states are weakly allowed. (In the parent cyclodecapentaene, the transitions are strongly forbidden, but the perturbations introduce some allowed character.) The B states are accessible from the ground state by fully allowed transitions. As shown in Table 1, the observed transitions are assigned, in order of increasing energy, to the L_b, L_a, B_b and B_a excited states.

There is little doubt about the assignment of the L_b and L_a transitions in the near ultraviolet, which have been studied extensively (Strickland 1974; Kahn 1978; Callis 1991). Auer (1973) studied the far-ultraviolet absorption and CD spectra of a number of indole derivatives. He resolved five or six Gaussian components in the spectrum of a number of derivatives. The Gaussian components were assigned to two (or possibly three) electronic transitions. The component at highest energy (190–198 nm) was assigned to the B_a transition on the basis of its intensity, energy and lack of vibrational fine structure. All (or most) of the remaining bands were assigned to vibronic components of the B_b transition.

The presence of another electronic transition was suggested by a weak, broad band which appeared just to the red of the B_b band in all the spectra. Auer suggested that this band, which is relatively much more significant in CD than in absorption, could be either an additional vibronic component of the B_b transition or a C band in the Platt (1949) nomenclature. Transitions from the ground state to C states are not only electrically forbidden but also magnetically forbidden. The substantially stronger contribution to CD than to absorption suggests that this long-wavelength feature is magnetically allowed and thus argues against both the B_b and C assignments. Moreover, π-electron-only calculations discussed below fail to indicate any $\pi\pi^*$ transitions lying between the L_a and B_b transitions in energy, and thus provide further evidence against the tentative C band assignment. The most likely explanation for the CD intensity is that all of the optically active derivatives studied are carboxylic acids, esters or amides and therefore have $n\pi^*$ transitions in the 220–230 nm region. Auer presented arguments against any significant carbonyl $n\pi^*$ contributions based upon: (1) identifying corresponding bands in absorption and CD; (2) strong similarities in effects of ionization of carboxylic and amino groups; and (3) solvent effects. All of these arguments are reasonable for the dominant bands, but become questionable for the very weak absorption feature on the long-wavelength edge of the main B_b band.

Another aspect of Auer's (1973) assignment may require revision. The Gaussian resolutions gave a band in

Table 1. Comparison of theory and experiment for indole transitions

Transition	Experiment [a]			Calculation I [b]			Calculation II [c]		
	λ	f [d]	θ [e]	λ	f [f]	θ	λ	f [f]	θ
L_b	282	0.01	49, 58 45, 60	304	0.004	45	284	0.007	80
L_a	269	0.11	−42, −30	270	0.200	−37	259	0.107	−56
B_b	214	0.68		225	0.700	25	213	0.807	15
B_a	200	–		212	0.118	−41	200	0.117	−44
				205	0.322	−56	193	0.187	−18
				201	0.061	39	190	0.399	−80
				197	0.113	−15	187	0.004	−61

[a] Yamamoto and Tanaka (1972) for 3-indolylacetic acid and (Gly-Trp) dihydrate, Philips and Levy (1986a) for indole, and Philips and Levy (1986b) for tryptamine

[b] Parameters of Goux et al. (1976)

[c] Parameters of Nishimoto and Forster (1965, 1966)

[d] Oscillator strengths estimated for aqueous solution of L-Trp (Yamamoto and Tanaka 1972)

[e] The first two numbers are the transition moment directions for 3-indolylacetic acid and Gly-Trp dihydrate, respectively (Yamamoto and Tanaka 1972). For the L_b band, the third and fourth numbers are the transition moment directions for indole (Philips and Levy 1986a) and for tryptamine (Philips and Levy 1986b), respectively. The angle θ is defined with respect to the long axis of indole, which is directed from the midpoint of the C_5–C_6 bond through C_2. Positive values correspond to clockwise rotations as shown in Fig. 1, i.e., away from N_1

[f] Theoretical oscillator strengths calculated as geometric mean of f_r and f_v, the dipole length and dipole velocity approximations (Hansen 1967), respectively

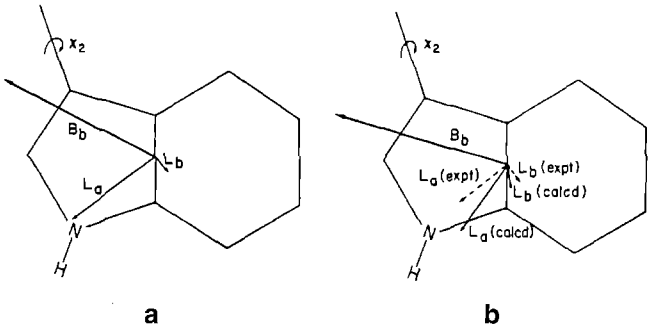

Fig. 1. a Theoretical transition moment directions calculated with the parameters of Goux et al. (1975). The experimental directions (Yamamoto and Tanaka 1972) for the L_b and L_a bands are not shown because they are essentially coincident with the theoretical directions. (Goux et al. adjusted parameters to obtain this fit.) **b** Transition moment directions calculated with Nishimoto and Forster (1965, 1966) parameters. Experimental directions for the L_b and L_a bands are shown for comparison as dashed arrows

the 205–215 nm region, observable in both absorption and CD. Although Auer assigned this band to a vibronic component of the B_b band, in most of the optically active derivatives the CD of this band is opposite in sign to that of the longer wavelength B_b components. In electrically forbidden transitions, it is not uncommon to observe vibronic components differing in sign (Weigang 1966), but such vibrations are not expected in strongly allowed transitions such as the indole B_b transition. Thus, Auer's results suggest that there may be an additional electronic transition between the B_b and B_a transitions.

Transition moment directions for the L_b and L_a transitions in the indole chromophore have been determined by polarized absorption measurements on single crystals of 3-indolylacetic acid and glycyl-L-tryptophan dihydrate (Yamamoto and Tanaka 1972). These experimental results are shown in Fig. 1. Recently, the L_b transition moment direction has been determined for indole (Philips and Levy 1986 a) and for tryptamine (Philips and Levy 1986 b) in the gas phase by rotationally resolved absorption spectroscopy on supercooled jets. Given the differences in environment and molecular structure, the polarization for the transitions in crystalline 3-indolylacetic acid ($+49°$ with respect to the long axis) and Gly-Trp ($+58°$) agree reasonably well with those for indole ($+45°$) and tryptamine ($+60°$) in the gas phase.

Methods

The present calculations require transition moment directions for the higher energy transitions, especially that of the B_b band, and also require transition monopole charges (Tinoco 1962) to evaluate the coupling between excited states within the chromophore and between transitions on different chromophores. These parameters have been obtained from π-electron MO calculation of the Pariser-Parr-Pople type (Murrell and Harget 1972). Two choices (Goux et al. 1976; Nishimoto and Forster 1965, 1966) of π-electron parameters were considered. The geometry for indole was taken from the crystal structure of 3-indolylacetic acid (Karle et al. 1964).

The system studied is a tryptophan side chain and the amide groups attached to the Trp C_α. It is thus equivalent to N-acetyl-L-Trp-NHMe. Rotational strengths and transition energies have been calculated using an exciton-like method (Tinoco 1962), in an origin-independent version (Goux and Hooker 1980) of the matrix method (Bayley et al. 1969). Most of the methods used in this calculation have been described in detail in previous papers (Woody 1968, 1978; Chen and Woody 1971). The transition monopole positions for the indole group were located at the atomic centers as were those for the amide $\pi\pi^*$ transition, and the monopole charges were calculated from the Nishimoto-Forster wavefunctions. The center for the indole transitions was the center of the $C_{\delta 2}-C_{\varepsilon 2}$ bond. The first six indole transitions were included, i.e., all of the ones indicated in Table 1, except the weak band at 187 nm. The first two transitions (L_b, L_a) were placed at the energies reported by Yamamoto and Tanaka (1972), and their transition dipole velocity magnitudes were adjusted to agree with the experimental oscillator strengths, but the transition dipole velocity directions were taken from the calculated transition dipole moments. The B_b transition was placed at 5.63 eV (220 nm) and the transition dipole velocity magnitude was adjusted to reproduce the observed oscillator strength (Yamamoto and Tanaka 1972). For the higher energy transitions, transition dipole velocity magnitudes were adjusted to give agreement with the theoretical oscillator strengths calculated as the geometric mean of the dipole length and dipole velocity oscillator strengths (Hansen 1967). The transition monopole charges calculated from the π-electron wavefunctions were multiplied by a factor of 0.789, which was the mean scaling factor required to produce agreement between the calculated transition dipole moments and those which reproduce the oscillator strengths as just described. (The range of scaling factors for the first six transitions was surprisingly narrow: 0.745 to 0.824.) The same scaling factor was applied to the transitions connecting excited states.

The values reported for the tryptophan B_b transition in this paper include the rotational strengths for the $n\pi^*$ transitions, which will not generally be resolved from those of the indole B_b transition that has been located at 220 nm in the calculations. The geometries of the model dipeptides were generated by the matrix methods of Ooi et al. (1967), as modified by McGuire et al. (1971) with respect to bringing the side-chain coordinate system into the backbone coordinate system. The standard peptide geometry of Momany et al. (1975) was used for the amide groups, for the geometry around C_α, and for the $C_\alpha-C_\beta$ and $C_\beta-C_\gamma$ bonds. The structure of the indole group was taken from that of 3-indolylacetic acid (Karle et al. 1964).

Dipeptide conformations from various regions of the Ramachandran map were considered: α_R ($-62°$, $-41°$) (Barlow and Thornton 1988); β ($-122°$, $+143°$) (Richardson et al. 1978); α_L ($+60°$, $+60°$); ($-120°$, $-70°$); ($-80°$, $-10°$); the poly (Pro) II region (P_{II}) ($-80°$, $+150°$); and the extended region ($-120°$, $+180°$). These regions were chosen not only because they sample the most heavily

populated regions of the Ramachandran map, but also because they have differing preferences for side-chain conformations according to the calculations of Lipkind and Popov (1971). For each backbone conformation, a number of side-chain conformations were considered, including *gauche*$^-$, *trans*, and *gauche*$^+$ conformers around the $C_\alpha - C_\beta$ bond, corresponding to $\chi_1 = 60°$, 180° and 300°, respectively. Various studies (Sasisekharan and Ponnuswamy 1971; Ponnuswamy and Sasisekharan 1971; Janin et al. 1978; Bhat et al. 1979; Benedetti et al. 1983; Ponder and Richards 1987; McGregor et al. 1987) indicate that the most favorable χ_2 value for aromatic amino acid side chains is 90°, with the range of χ_2 being most restricted for $\chi_1 = 60°$ and less restricted for the *trans* and *gauche*$^+$ conformers. Following Sasisekharan and Ponnuswamy (1971), we have used $\chi_2 = 90°$ and 270° for $\chi_1 = 60°$; $\chi_2 = 60° - 120°$ and $240° - 300°$ in 30° intervals for $\chi_1 = 180°$; and $\chi_2 = 60° - 150°$ and $240° - 330°$ in 30° intervals for $\chi_1 = 300°$.

Calculations have also been performed on the 15 proteins from a widely used data base for the analysis of protein structure by circular dichroism (Hennessey and Johnson 1981). Each of these proteins contains at least one tryptophan. The coordinates used were obtained from the Protein Data Bank (Bernstein et al. 1977; Abola et al. 1987). The proteins considered were: γ-chymotrypsin A (bovine) (Cohen et al. 1981); cytochrome *c* (tuna) (Takano and Dickerson 1980); elastase (tosyl, porcine) (Sawyer et al. 1978); flavodoxin (oxidized, *Clostridium* MP) (Smith et al. 1977); D-glyceraldehyde-3-phosphate dehydrogenase (lobster) (Moras et al. 1975); hemoglobin (aquomet, equine) (Ladner et al. 1977); lactate dehydrogenase (dogfish, M_4 apo) (Abad-Zapatero et al. 1987); lysozyme (chicken) (Herzberg and Sussman 1983); myoglobin (sperm whale, aquomet) (Watson 1969); papain (papaya, cysteinyl) (Drenth et al. 1976); prealbumin (human) (Blake et al. 1978); rubredoxin (*Clostridium pasteurianum*, oxidized) (Watenpaugh et al. 1980); subtilisin (*Bacillus amyloliquefaciens*) (Alden et al. 1971); thermolysin (*B. thermoproteolyticus*) (Holmes and Matthews 1982); triosephosphate isomerase (chicken) (Banner et al. 1976).

The transition monopoles were placed at the atomic positions given by the crystal coordinates, except for the amide nπ* monopoles, which were placed at standard positions (Woody 1968) around the carbonyl oxygen. The transition dipole velocity vectors and the magnetic dipole transition moment of the amide nπ* transition were transformed from the standard peptide and indole coordinate systems into the crystal coordinate system by a matrix transformation. Only the interaction of each indole side chain with the two amides bonded to its C_α was considered.

Results and discussion

The first problem to consider is the choice of MO parameters. Goux et al. (1976), starting from literature values, adjusted their parameters to obtain close agreement with the experimental transition moment directions of Yamamoto and Tanaka (1972). The results using the parameters of Goux et al. (1976) are shown in Table 1. These results agree well with those reported by Goux et al., with minor differences attributable to slightly different geometries and to less extensive configuration interaction in the present calculation (10 low-energy singlet excited configurations vs. all 20 singly excited configurations). As Goux et al. had shown, these parameters give excellent agreement with the experimental transition moment directions for the L_b and L_a bands (Yamamoto and Tanaka 1972). However, the parameters of Goux et al. (1976) predict a very congested spectrum just above 200 nm, with four transitions between 197 and 212 nm. Therefore, the parameters of Nishimoto and Forster (1965, 1966), which generally work well in predicting transition energies and intensities in heterocyclic systems, were also used. The results from this calculation are shown in Fig. 1 and Table 1, in comparison with experiment and with the results from the Goux et al. parameters. Although the L_b, and L_a transition moment directions are not given as well with the Nishimoto and Forster parameters, the pileup of transitions above 200 nm is eliminated. The Goux et al. parameters place the B_a transition at 205 nm, whereas the Nishimoto-Forster parameters place it at 190 nm, in considerably better agreement with Auer's (1973) experimental data. Depending on the parameter choice, one or two transitions are predicted to lie between the B_b and B_a bands, which is consistent with the present interpretation of Auer's results. (The additional transition at 193 nm with the Nishimoto and Forster parameters would not be resolved from the much stronger B_a band at 190 nm.) Overall, the Nishimoto-Forster parameters give a better account of the far-ultraviolet spectrum of indole and therefore these parameters have been used in the treatment of the CD of tryptophan-containing peptides.

The calculated B_b rotational strengths for the various dipeptide conformers are shown in Table 2. The first striking feature of these results is that many of the conformers give rotational strengths, R, which are greater than 0.2 DBM (Debye-Bohr magneton, 1 DBM = 0.9273 $\times 10^{-38}$ cgs units) in magnitude. Assuming a band width of 9.0 nm, the maximum molar ellipticity is 1.9×10^5 R. Thus, a rotational strength of 0.2 DBM corresponds to $[\Theta]_{max} = 38\,000$ deg cm^2/dmol. This is comparable (but opposite in sign) to the CD contribution of the nπ* transition in an α-helical peptide group. Therefore, many of these conformers are predicted to have CD bands of substantial magnitude, with the strongest bands with $[\Theta]_{max} \sim 10^5$ deg cm^2/dmol.

Although more than half the conformers give rotational strengths of the order of 0.2 DBM or larger in magnitude, there are a number of conformers which give a net B_b rotational strength less than 0.2 DBM in magnitude. In most cases, however, the small net rotational strength results from approximate cancellation of two large rotational strengths of opposite sign that result from mixing of the indole B_b transition with the two amide nπ* transitions. For example, for the α_R conformer with $(\chi_1, \chi_2) = (60°, 90°)$, the net B_b rotational strength is predicted to be 0.073 DBM. However, this is a resultant of three transitions at 220.56, 220.04 and 219.95 nm with rotational

Table 2. Calculated tryptophan B_b rotational strengths [a] in N-AcTrpNHMe

Backbone conformation	Side-chain conformation [b]							
	(60, 90)	(180, 60)	(180, 90)	(180, 120)	(300, 60)	(300,90)	(300, 120)	(300, 150)
α_R	−0.197	0.207	−0.064	−0.235	−0.063	0.020	0.217	0.413
(−62, −41)	−0.260	0.553	0.542	0.299	0.449	0.381	0.477	0.495
β	0.657	0.513	−0.013	−0.519	−0.380	−0.390	−0.274	−0.058
(−122, +143)	−0.687	−0.318	−0.047	0.180	0.725	0.395	0.028	−0.246
α_L	0.512	−0.174	−0.065	−0.485	−0.156	−0.389	−0.484	−0.382
(60, 60)	−0.071	−0.220	−0.018	−0.009	−0.273	−0.351	−0.466	−0.416
	1.086	0.384	0.129	−0.338	−0.285	−0.432	−0.274	0.103
−120, −70	−0.471	−0.304	0.161	0.424	0.746	0.246	−0.032	−0.022
	−0.280	0.365	0.063	−0.037	−0.179	−0.149	0.028	0.142
−80, −10	−0.033	0.238	0.319	0.288	0.832	0.815	0.812	0.656
P_{II}	0.017	0.289	−0.247	−0.659	−0.226	−0.088	0.183	0.453
(−80, +150)	−0.519	0.386	0.470	0.398	0.888	0.746	0.646	0.470
	0.611	0.567	0.175	−0.115	−0.121	−0.259	−0.327	−0.205
−120, +180	−0.281	−0.659	−0.353	0.084	1.057	0.744	0.270	−0.093

[a] Includes rotational strengths of indole B_b and peptide $n\pi^*$ transitions. In Debye-Bohr magnetons (1 DBM = 0.9273×10^{-38} cgs units)
[b] The upper number in each entry is for the (χ_1, χ_2) pair at the top of the column. The lower number is for $(\chi_1, \chi_2 + 180)$

strengths of −0.527, 0.401 and 0.200 DBM, respectively. Because the splittings are small compared with the band width and because there is a net rotational strength, CD spectra calculated (data not shown) from the theoretical rotational strengths do not exhibit the classical couplet shape (Schellman 1968; Bayley 1973).

Does the choice of 220 nm for the B_b band position affect the results significantly? Calculations of rotational strength and CD were performed for two alternative wavelengths. The absorption maximum for 3-indolylacetic acid in water is at 214 nm (Yamamoto and Tanaka 1972), whereas poly(Trp) exhibits a CD maximum near 225 nm (Cosani et al. 1968; Peggion et al. 1968). Calculations with either of these wavelengths for the B_b transition gave net rotational strengths and CD spectra which differed only quantitatively. The magnitudes were generally greater when the B_b band was placed at 214 nm and least for 225 nm. This trend results from the fact that the principal source of B_b rotational strength is through mixing with higher energy indole and peptide $\pi\pi^*$ transitions.

A second striking feature of the results shown in Table 2 is that there are generally large differences associated with rotating about the $C_\beta - C_\gamma$ bond (χ_2) by 180°. In nearly all cases where the rotational strengths are large in magnitude for both conformers differing in χ_2 by 180°, the B_b band has rotational strengths opposite in sign. Dipeptides in the α_L region are exceptional in giving negative rotational strengths for all but one side-chain conformation.

Is there any preference for positive over negative B_b bands, or vice versa? The number of positive and negative entries in Table 2 are essentially equal. However, each main-chain conformation will have a preference for particular side-chain conformations (Lipkind and Popov 1971; Janin et al. 1978; Benedetti et al. 1983; McGregor et al. 1987). In Table 3, the preferences of various main-chain conformations for particular χ_1 values are taken into consideration in calculating average B_b rotational strengths. The preferences inferred by Lipkind and Popov (1971) are used here, as these are the most complete and explicit ones available, although based upon limited data. They are consistent with the results of subsequent studies with larger data bases (Janin et al. 1978; Benedetti et al. 1983; McGregor et al. 1987).

Table 3. Calculated tryptophan B_b rotational strengths [a] for most favorable conformations

Backbone conformation	Favored χ_1 [b]	$\chi_2 = 90°$	$\chi_2 = 270°$	Average over χ_2 [c]	
				Unweighted	Weighted
α_R	180	−0.0636	+0.5421	0.2172	0.1347
β	300	−0.3900	+0.3952	−0.0249	−0.1084
α_L	300	−0.3894	−0.3512	−0.3649	−0.3610
−120, −70	300	−0.4315	+0.2460	+0.0062	−0.0698
−80, −10	60	−0.2801	−0.0329	−0.1565	−0.1977
−80, +150	180	−0.2466	0.4696	0.1060	0.0022
−120, +180	60	0.6110	−0.2808	0.1651	0.3137

[a] Includes rotational strengths of indole B_b and peptide $n\pi^*$ transition. In DBM
[b] Based on calculations of Lipkind and Popov (1971)
[c] Unweighted average includes all χ_2 for the favored χ_1, with the same weight. In the weighted average, rotational strengths for $\chi_2 > 180°$ were assigned a weighting factor of 0.5 while those for $\chi_2 < 180°$ were given unit weight

Except for the (−120, +180) region, the B_b rotational strength is negative for the favored χ_1 values when $\chi_2 = 90°$. The band is predicted to be positive for $\chi_2 = 270°$ and the favored χ_1 value in four of the seven conformations considered, and these include the most populated regions of the Ramachandran map. The unweighted averages over χ_2 are positive for the α_R, P_{II} and extended regions and very weakly negative for the β region. Only the lightly

populated α_L and bridge (-80, -10) regions give significant negative B_b bands.

Analyses of protein structures (Janin et al. 1978; Bhat et al. 1979; McGregor et al. 1987) indicate that tryptophan side chains with χ_2 between 0° and 180° occur about twice as frequently as those with χ_2 between 180° and 360°. The smaller sample of tryptophan residues in globular proteins considered in the present work exhibits a ratio of ca. 3:1. The weighted averages given in Table 3 use the 2:1 weighting for χ_2 implied by the protein structural data. When this preference is considered, the three most populated regions give positive (α_R), negative (β) and very weakly positive (P_{II}) B_b bands. Only the improbable α_L region gives a strongly negative B_b band. Overall, the weighted average could yield either a positive or negative B_b band, depending on the relative weights of the α_R and β regions. Thus, our calculations do not make a strong prediction for the sign of the Trp B_b band, in contrast to the L_a bands of Phe and Tyr (Woody 1978).

Experimentally, the CD spectrum of N-acetyl-L-tryptophanamide in water (Shiraki 1970) has a positive band at 227 nm with $[\Theta]_{227} = 12\,900$ deg cm^2/dmol, a crossover at ~217 nm, a negative shoulder near 212 nm, and a negative maximum at 196 nm with $[\Theta]_{196} = -10\,800$ deg cm^2/dmol. A similar spectrum is observed for Glu-Trp (Brahms and Brahms 1980). All of the tryptophan derivatives studied by Auer (1973) also exhibited a positive CD band in the 220–230 nm region. The present calculations, therefore, imply a predominance of peptide conformers in the α_R relative to the β region. Alternatively, the bias against $\chi_2 > 180°$ may be minimal in these peptides, in which case the unweighted average is more appropriate and the α_R and PP_{II} regions are predicted to give rise to moderately strong positive B_b bands, whereas the β region gives a weakly negative contribution.

The results for the globular proteins are shown in Table 4. The limits on these calculations must be kept clearly in mind. Only nearest-neighbor interactions are included. The interactions of each tryptophan side chain with other amides than those attached to its α carbon, and with other chromophoric side chains, are ignored. It is likely that these non-nearest neighbor contributions are of comparable, if not greater, importance in determining the far-ultraviolet CD of the tryptophan side chains. Nevertheless, the present calculations can give some idea of the possible strength of such effects.

The protein calculations again show a bias toward positive B_b contributions from tryptophan. Although nine of the 15 proteins have overall negative contributions, six of these are quite weak, while those proteins with positive B_b bands give generally stronger bands. Comparison of the average magnitudes with the net rotational strengths shows that there is substantial cancellation. For example, elastase has a net B_b rotational strength which is close to zero, but the average magnitude is 0.44 DBM. This corresponds to $[\Theta]_{max}$ values of $\sim 5 \times 10^4$.

Although most proteins have negative CD bands near 220 nm, dominated by α-helix and/or β-sheet contributions, a few proteins have positive CD at 220 nm, with maxima between 220 and 235 nm. Table 5 gives data on some of these proteins. It is not certain that aromatic groups are responsible for these positive CD bands in all cases (see below), but the position of the bands is consistent with an assignment of the B_b transition of tryptophan or the L_a band of tyrosine, or both. For this reason, Table 5 contains a column reporting the ellipticity per aromatic group, assuming that all tryptophans and tyrosines contribute equally. It can be seen that this value ranges from ~3500 deg cm^2/dmol to ~80 000 deg cm^2/dmol. Such values are well within the range predicted in this study for tryptophan side chains. In a previous study (Woody 1978), calculations on the L_a band of tyrosine indicated possible contributions of up to ~0.5 DBM, corresponding to a molar ellipticity of ~65 000 deg cm^2/dmol. Thus, the anomalous CD of the proteins in Table 5 can be accounted for by aromatic side chain contributions resulting solely from nearest-neighbor interactions. However, those with very large values per aromatic side chain, such as avidin, require a large degree of reinforcement among the side chains and only weak negative peptide contributions. Of course, contributions of chromophores more distant in the primary structure but near in the tertiary structure can modify this picture.

The assignment to aromatic side chains of the positive CD bands near 230 mm in snake neurotoxins and cardiotoxins has been excluded (Dufton and Hider 1983; Grognet et al. 1988; Hider et al. 1988). Tyr 25 and Trp 29 (erabutoxin numbering) are strongly, but not completely, conserved among these toxins. The 228 nm band is observed in a number of toxins which lack the Trp homologous to Trp 29 and the few toxins lacking the Tyr homologous to Tyr 25. Hider et al. (1988) have suggested that the 228 nm band is largely due to the disulfides, which are completely conserved in these toxins.

Table 4. Calculated tryptophan B_b rotational strengths [a] in globular proteins

Protein	R	n [b]	$\langle R \rangle$	$\langle \lvert R \rvert \rangle$	PDB file [c]
Chymotrypsin	−0.2200	8	−0.0275	0.3451	2gch
Cytochrome c	2.1560	4	0.5390	0.5390	3cyt
Elastase	−0.0218	7	−0.0031	0.4392	1est
Flavodoxin	−0.7650	3	−0.2550	0.3000	3fxn
G3PDH [d]	−0.0576	6	−0.0096	0.3150	1gpd
Hemoglobin	0.6753	3	0.2251	0.2833	2mhb
LDH [e]	0.7381	6	0.1230	0.2309	6ldh
Lysozyme	−0.0746	6	−0.0124	0.2141	7lyz
Myoglobin	0.3602	2	0.1801	0.3323	1mbn
Papain	−0.8140	5	−0.1628	0.2369	2pad
Prealbumin	0.4040	4	0.1010	0.2662	2pab
Rubredoxin	−0.2920	1	−0.2920	0.2920	5rxn
Subtilisin	0.5199	3	0.1733	0.1754	1sbt
Thermolysin	−0.0559	3	−0.0186	0.6241	3tln
TIM [f]	−0.6745	10	−0.0675	0.3201	1tim

[a] Includes indole B_b and amide $n\pi^*$ rotational strengths. In DBM
[b] Number of tryptophan residues in asymmetric unit of crystal
[c] File name in the Protein Data Bank for the crystal structure used in the calculation
[d] Glyceraldehyde-3-phosphate dehydrogenase
[e] Lactate dehydrogenase
[f] Triose phosphate isomerase

Table 5. Positive CD bands in proteins (220–235 nm)

Protein	λ_{max} (mm)	$[\Theta]_{max}$ [a]	n_{Tyr} [b]	n_{Trp} [c]	$\frac{[\Theta]_{max}}{n_{Tyr}+n_{Trp}}$
Agglutinin (wheat germ)	223	470 000	7	1	59 000 [d]
Avidin	228	410 000	1	4	82 000 [e]
Cobrotoxin	228	219 000	2	1	73 000 [f]
γ-Crystallin IV	234	138 000	16	4	7 000 [g]
DNase (acid)	225	63 000	12	6	3 500 [h]
Erabutoxin b	228	100 000	1	1	50 000 [i]
Factor H	230	3 300 000	58	36	35 000 [j]
Ferredoxin	227	225 000	2	2	56 000 [k]
Fibronectin	228	8 800 000	146	88	38 000 [l]
Gene 5 protein	228	17 000	5	0	3 400 [m]
β_2-Glycoprotein I	235	199 000	12	4	12 000 [n]
Hemopexin (apo)	231	117 000	12	17	4 000 [o]
Hevein	221	190,000	1	2	63 000 [d]
High-potential iron protein	228	460 000	3	3	77 000 [p]
Myotoxin a	225	12 500	1	1	6 300 [q]
α-Neurotoxin	228	100 000	1	1	50 000 [r]
Neocarzinostatin	223	96 000	1	2	32 000 [s]
Ribonuclease Sa	235	160 000	7	0	23 000 [t]
B-Ricin	232	870 000	9	6	58 000 [u]
Trypsin inhibitor (Kunitz soybean)	226	430 000	4	2	72 000 [v]
Trypsin inhibitor	227	229 000	11	1	19 000 [w]

[a] Per subunit or per protein
[b] Number of tyrosine residues per subunit or per protein
[c] Number of tryptophan residues per subunit or per protein
[d] Rodriguez-Romero et al. (1989)
[e] Green and Melamed (1966)
[f] Yang et al. (1968)
[g] Mandal et al. (1985)
[h] Timasheff and Bernardi (1970)
[i] Menez et al. (1976)
[j] Discipio and Hugli (1982)
[k] Ohmori (1984)
[l] Österlund et al. (1985)
[m] Day (1973)
[n] Lee et al. (1983)
[o] Morgan and Smith (1984)
[p] Przysiecki et al. (1985)
[q] Cameron and Tu (1977)
[r] Menez et al. (1976)
[s] Maeda et al. (1973)
[t] Kéry et al. (1986)
[u] Wawrzynczak et al. (1988)
[v] Ikeda et al. (1968)
[w] Gruen et al. (1984)

The CD spectrum of the bacterial ribonuclease barnase shows a prominent negative band at 231 nm (Vuilleumier et al. 1993). Vuilleumier et al. have mutated each of the three Trp and each of the seven Tyr residues to Phe. Difference CD spectra between the mutant and wild-type proteins lead to the conclusion that Trp 94 and Tyr 24 contribute ca. $-180\,000$ deg cm^2/dmol and ca. $-110\,000$ deg cm^2/dmol, respectively, to the 231 nm CD band. Trp 35 makes a contribution of ca. $+140\,000$ deg cm^2/dmol at 224 nm, while Tyr 90 and 97 give rise to CD bands at 221 nm with amplitudes of ca. $+250\,000$ and $-110\,000$ deg cm^2/dmol, respectively. Further in the ultraviolet, difference bands of comparable and even greater magnitude are detected, but the analysis is more complex in this region because the Phe residues also may contribute here, as well as the peptide groups. The results for the Trp B_b bands are comparable in magnitude to those predicted in this work. It must be emphasized again, however, that coupling of the Trp B_b band with other peptides than the nearest neighbors and with other aromatic groups may actually dominate the B_b CD contributions in many cases.

Two cases in which coupling of the Trp B_b transition with groups other than flanking peptides have recently been documented. Kuwajima et al. (1991) have reported that the difference CD spectrum between wild-type *E. coli* dihydrofolate reductase and the mutant in which Trp 74 is replaced by a leucine has a strong positive band at 230 nm and a negative band at 220 nm (WT-mutant). The overall amplitude of this couplet is ca. 2.3×10^3 deg cm^2/dmol residue or 360 000 per protein. Kuwajima et al. attributed this couplet to an exciton interaction between the B_b bands of Trp 74 and Trp 47, which are in close proximity in the structure of *E. coli* DHFR. This assignment is supported by explicit calculations (Grishina and Woody to be published).

The CD spectrum of the filamentous phage fd qualitatively resembles that of an α-helix, consistent with the high helix content of the coat protein. However, the ratio of the 222 nm band to that of the 208 nm band is close to 1.5, rather than 1.0 as normally observed with α-helices. Arnold et al. (1992) have shown that oxidation by N-bromosuccinimide of the lone Trp per coat protein molecule leads to a decrease of the 222 nm amplitude and an increase in the 208 nm band, i.e., a normalization of the α helix spectrum. The difference spectrum between the unmodified and modified virus CD thus shows a strong couplet with a negative peak at 224 nm and a positive peak at 210 nm. The overall amplitude of the couplet is estimated to be ca. $+10$ deg cm^2/dmol. The difference CD bands are substantially to the blue from those in the dihydrofolate reductase. This argues against exciton coupling between Trp B_b bands, and data on the capsid structure indicate that the Trp residues on different subunits are too far apart to give rise to a significant exciton effect (K. Dunker, private communication). However, Trp 26 on one subunit is expected to lie close to Phe 42 on a neighboring subunit (Marvin et al. 1994) and the band positions in the couplet would be compatible with a Trp B_b–Phe L_a interaction. Detailed calculations will be required to ascertain whether such an interaction can give rise to the extraordinary CD magnitude observed.

Although most methods (Yang et al. 1986; Johnson 1988; Woody 1994) for secondary structure analysis of proteins from CD do not explicitly consider aromatic contributions, three methods have attempted to take them into account. Brahms and Brahms (1980) measured the CD of model dipeptides for Trp, Phe and Tyr, e.g., Glu-Trp, and combined these spectra with amino acid composition data to yield a simple correction to the observed spectrum. Although this led to a slightly better least-squares fit to the spectrum in some cases, as manifested by a smaller r.m.s. deviation from the experimental curve, the content of various secondary structural elements changed by only a few percent at most. Furthermore, it is not clear that these changes led to improved agreement with X-ray data. It seems unlikely that a simple dipeptide can serve as an adequate model for all of the aromatic chromophores in a protein.

Bolotina and Lugauskas (1986) have extended the nonlinear least squares method to include contributions of aromatic chromophores. The CD spectra of a set of proteins of known structure are measured at regular

intervals. The observed CD spectrum of a protein is considered to be made up of a contribution from each secondary structural type, weighted by the fraction of that structural type in the protein, plus aromatic contributions. The aromatic contributions are unique for each protein and are taken to consist of three bands, with wavelengths in the ranges 190–210, 210–226 and 226–235 nm. Each of the bands is taken to have a shape function which is a log-normal distribution (Siano and Metzler 1969), and thus each band requires four parameters. An iterative nonlinear least squares procedure was used to obtain the peptide reference spectra for the structural types, assumed common to all proteins, and the twelve parameters describing the aromatic contribution, unique to each protein. Proteins of unknown conformation were analyzed to obtain the unique aromatic contribution and the fractions of secondary structural elements.

As gauged by improved agreement between the CD analyses and X-ray diffraction for proteins outside the basis set, the method of Bolotina and Lugauskas (1986) represents an improvement over the analysis omitting the aromatic contributions. The allowance for unique aromatic contributions for each protein represents a major advance which may provide useful information about these contributions, as well as improving the accuracy of secondary structural estimates from CD.

However, there are several concerns about the Bolotina and Lugauskas (1986) method. The large increase in the number of parameters raises questions about the stability and convergence of the least squares procedure. The analysis constrains the secondary structure fractions to be positive and to sum to one, as do nearly all earlier methods. However, most recently developed methods follow Hennessey and Johnson (1981) and do not apply such constraints. Instead, the extent to which the unconstrained secondary structural fractions satisfy these conditions provides useful criteria for a valid analysis. No such test is available in the Bolotina-Lugauskas method and it is possible that the additional parameters could yield a good fit to the experimental CD spectrum, but the derived fractions could be in error.

Perczel et al. (1992) applied their convex constraint analysis (CCA) (Perczel et al. 1991) to a set of proteins which included four proteins rich in β-sheets, in addition to the 18 proteins used in their initial work. The CCA method does not require any input data from X-ray structures. Instead, the CD data are treated as vectors which are subjected to rotations that yield a set of pure component spectra, the number of which can be varied. When the β-protein-enriched data set was analyzed to obtain five components, four of the components were spectra resembling secondary structural elements such as the α-helix, antiparallel β-sheets, etc. One component, however, showed only one significant feature, a positive band centered at 230 nm. Perczel et al. suggested that this band arises from aromatic and disulfide side chain groups and showed that its amplitude in the CD spectra of the basis set proteins showed a modest correlation ($r = 0.48$) with the fraction of aromatic + disulfide-linked cysteine residues. This method of correcting for aromatic contributions will break down in cases where the net contribution for a specific protein is negative, since the coefficient for each pure component is restrained to be prositive.

Several recently developed methods (van Stokkum et al. 1990; Sreerama and Woody 1993) use the variable selection principle introduced by Manavalan and Johnson (1987). In this approach, various combinations of protein CD spectra are used to fit the spectrum of one unknown protein, rather than a single set. This has the advantage that proteins which have CD features in common with the unknown protein are given additional weight in the analysis while those which have very different features are deleted from the basis set. Thus if one or more proteins in the total basis set have aromatic CD contributions similar to those in the spectrum of the unknown protein, the variable selection method will weight that (those) proteins more heavily in the analysis. If none of the proteins in the initial basis set have such contributions, the variable selection method will not lead to an improved result. In such cases, if the aromatic feature is very prominent, e.g., in the proteins listed in Table 5, the analysis can generally be recognized as flawed by the failure of the secondary structure fractions to all be positive and/or to sum to one.

From the present work, it is clear that tryptophans can make a significant contribution to the CD of proteins in the far ultraviolet. In general, this is likely to substantially perturb the CD spectrum only in cases where the peptide contribution is weak, in particular, in proteins with low helix content. Unlike the L_a bands of tyrosine and phenylalanine (Woody 1978), there is not a clear tendency for the B_b band of tryptophan to be positive when only nearest-neighbor interactions are considered. Nevertheless the anomalous CD spectra of certain proteins which exhibit positive CD bands near 225 nm are probably due, at least in part, to Trp B_b contributions. For proteins with apparently normal CD spectra, the extent to which these contributions may interfere with secondary structure analysis, and how best to recognize and correct for such effects, remains to be elucidated.

Acknowledgements. This work was supported by a grant from the U.S. Public Health Service, GM 22994. I am also grateful to the Colorado State University Computer Center for making free computer time available.

References

Abad-Zapatero C, Griffith JP, Sussman JL, Rossmann M (1987) Refined crystal structure of dogfish M_4 apo-lactate dehydrogenase. J Mol Biol 198:455–467

Abola EE, Bernstein FC, Bryant HH, Koetzle TF, Weng J (1987) Protein data bank, in: Allen FH, Bergerhoff G, Sievers R (eds) Crystallographic databases – Information content, software systems, scientific applications, Data Commission, International Union of Crystallography, Bonn Cambridge Chester, pp 107–132

Alden RA, Birktoft JJ, Kraut J, Robertus JD, Wright CS (1971) Atomic coordinates for subtilisin BPN′ (or Novo). Biochem Biophys Res Commun 45:337–344

Arnold GE, Day L, Dunker AK (1992) Tryptophan contributions to an unusual circular dichroism spectrum of the fd phage. Biochemistry 31:7948–7956

Auer HE (1973) Far-ultraviolet absorption and circular dichroism spectra of L-tryptophan and some derivatives. J Am Chem Soc 95:3003–3011

Banner PW, Bloomer AC, Petsko GA, Phillips DC, Wilson IA (1976) Atomic coordinates for triose phosphate isomerase from chicken muscle. Biochem Biophys Res Commun 72:146–155

Barlow DJ, Thornton JM (1988) Helix geometry in proteins. J Mol Biol 201:601–619

Bayley PM (1973) The analysis of circular dichroism of biomolecules. Progr Biophys Mol Biol 2:1–76

Bayley PM, Nielsen EB, Schellman JA (1969) The rotatory properties of molecules containing two peptide groups: Theory. J Phys Chem 73:228–243

Benedetti E, Morelli G, Nemethy G, Scheraga JA (1983) Statistical and energetic analysis of side-chain conformations in oligopeptides. Int J Pept Protein Res 22:1–15

Bernstein FC, Koetzle TF, Williams GJB, Meyer EF Jr, Brice MD, Rodgers JR, Kennard O, Shimanouchi T, Tasumi M (1977) The protein data bank: a computer-based archival file for macromolecular structures. J Mol Biol 112:535–542

Bhat TN, Sasisekharan V, Vijayan M (1979) An analysis of side-chain conformation in proteins. Int J Pept Protein Res 13:170–184

Blake CCF, Geisow MJ, Oatley SJ, Rerat B, Rerat C (1978) Structure of prealbumin, secondary, tertiary and quarternary interactions determined by Fourier refinement at 1.8 Å. J Mol Biol 121:339–356

Bolotina IA, Lugauskas VYu (1986) Determination of the secondary structure of proteins from the circular dichroism spectra. IV. Consideration of the contribution of aromatic amino acid residues to the circular dichroism spectra of proteins in the peptide region. Mol Biol (Engl. Transl.) 19:1154–1166

Brahms S, Brahms J (1980) Determination of protein secondary structure in solution by vacuum ultraviolet circular dichroism. J Mol Biol 138:149–178

Callis PR (1991) Molecular orbital theory of the ^1L_b and ^1L_a states of indole. J Chem Phys 95:4230–4240

Cameron DL, Tu AT (1977) Characterization of myotoxin a from the venom of prairie rattlesnake (Crotalus viridus viridus). Biochemistry 16:2546–2553

Chen AK, Woody RW (1971) A theoretical study of the optical rotatory properties of poly-L-tyrosine. J Am Chem Soc 93:29–37

Cohen GH, Silverton EW, Davies DR (1981) Refined crystal structure of γ-chymotrypsin at 1.9 Å resolution. Comparison with other pancreatic serine proteases. J Mol Biol 148:449–479

Cosani A, Peggion E, Verdini AS, Terbojevich M (1968) Far ultraviolet optical rotatory properties of poly-L-tryptophan. Biopolymers 6:963–971

Day LA (1973) Circular dichroism and ultraviolet absorption of a deoxyribonucleic acid binding protein of filamentous bacteriophage. Biochemistry 12:5329–5339

Discipio RG, Hugli TE (1982) Circular dichroism studies of human factor H. A regulatory component of the complement system. Biochim Biophys Acta 709:58–64

Drenth J, Kalk KH, Swen HM (1976) Binding of chloromethylketone substrate analogues to crystalline papain. Biochemistry 15:3731–3738

Dufton MJ, Hider RC (1983) Conformational properties of the neurotoxins and cytotoxins isolated from elapid snake venoms. CRC Crit Rev Biochem 14:113–171

Goux WJ, Hooker TM, Jr (1980) Chiroptical properties of proteins. 1. Near-ultraviolet circular dichroism of ribonuclease S. J Am Chem Soc 102:7080–7087

Goux WJ, Kadesch TR, Hooker TM, Jr (1976) Contribution of side-chain chromophores to the optical activity of proteins: Model compound studies. IV. The indole chromophore of yohimbinic acid. Biopolymers 15:977–997

Green NM, Melamed MD (1966) Optical rotatory dispersion, circular dichroism and far-ultraviolet spectra of avidin and streptavidin. Biochem J 100:614–621

Grognet JM, Ménez A, Drake A, Hayashi K, Morrison IEG, Hider RC (1988) Circular dichroic spectra of elapid cardiotoxins. Eur J Biochem 172:383–388

Gruen LC, Tao Z-J, Kortt AA (1984) Stability and physicochemical properties of a trypsin inhibitor from winged bean seed (*Psophocarpus tetragonolobus* (L) DC). Biochim Biophys Acta 791:285–293

Hansen AE (1967) Correlation effects in the calculation of ordinary and rotatory intensities. Mol Phys 13:425–431

Hennessey JP, Jr, Johnson WC, Jr (1981) Information content in the circular dichroism of proteins. Biochemistry 20:1085–1094

Herzberg O, Sussman JL (1983) Protein model building by the use of a constrained-restrained least-squares procedure. J Appl Crystallogr 16:144–150

Hider RC, Drake AF, Tamiya N (1988) An analysis of the 225–230 nm CD band of elapid toxins. Biopolymers 27:113–122

Holmes MA, Matthews BW (1982) Structure of thermolysin refined at 1.6 Å resolution. J Mol Biol 160:623–639

Ikeda K, Hamaguchi K, Yamamoto M, Ikenaka T (1968) Circular dichroism and optical rotatory dispersion of trypsin inhibitors. J Biochem 63:521–531

IUPAC-IUB Commission on Biochemical Nomenclature (1976) Abbreviations and symbols for the description of the conformation of polypeptide chains. Tentative rules (1969) in: Fasman GD (ed) Handbook of Biochemistry and Molecular Biology, 3rd edn, vol. I. CRC Press, Cleveland, pp 59–74

Janin J, Wodak S, Levitt M, Maigret B (1978) Conformation of amino acid side chains in proteins. J Mol Biol 125:357–386

Johnson WC, Jr (1988) Secondary structure of proteins through circular dichroism spectroscopy. Annu Rev Biophys Biophys Chem 17:145–166

Kahn PC (1978) The interpretation of near-ultraviolet circular dichroism. Methods Enzymol 61:339–378

Karle IL, Britts K, Gum P (1964) Crystal and molecular structure of 3-indolylacetic acid. Acta Crystallogr 17:496–499

Kéry V, Bystrický S, Ševčik J, Zelinka J (1986) Circular dichroism of the guanyloribonuclease Sa and its complex with guanosine-3′-phosphate. Biochim Biophys Acta 869:75–80

Kuwajima K, Garvey EP, Finn BE, Matthews CR, Sugai S (1991) Transient intermediates in the folding of dihydrofolate reductase as detected by far-ultraviolet circular dichroism spectroscopy. Biochemistry 30:7693–7703

Ladner RC, Heidner EG, Perutz MF (1977) The structure of horse methaemoglobin at 2.0 Å resolution. J Mol Biol 114:385–414

Lee NS, Brewer HB, Jr, Osborne JC, Jr (1983) β_2-glycoprotein I. Molecular properties of an unusual apolipoprotein, apoliprotein H. J Biol Chem 258:4765–4770

Lipkind GM, Popov EM (1971) Conformational states of amino acid residues in proteins. Side chains. Mol Biol (Engl. Transl.) 5:532–542

Maeda H, Shiraishi H, Onodera S, Ishida N (1973) Conformation of antibiotic protein, neocarzinostatin, studied by plane polarized infrared spectroscopy, circular dichroism and optical rotatory dispersion. Int J Pept Protein Res 5:19–26

Manavalan P, Johnson WC, Jr (1987) Variable selection method improves the prediction of protein secondary structure from circular dichroism spectra. Anal Biochem 167:76–85

Mandal K, Bose SK, Chakrabarti B, Siezen RJ (1985) Structure and stability of γ-crystallins, I. Spectroscopic evaluation of secondary and tertiary structure in solution. Biochim Biophys Acta 832:156–164

McGregor MJ, Islam SA, Sternberg MJE (1987) Analysis of the relationship between side-chain conformation and secondary structure in globular proteins. J Mol Biol 198:295–310

McGuire RF, Vanderkooi G, Momany FA, Ingwall RT, Crippens GM, Lotan N, Tuttle RW, Kashuba KL, Scheraga HA (1971) Determination of intermolecular potentials from crystal data. II. Crystal packing with applications to poly (amino acids). Macromolecules 4:112–124

Menez A, Bouet F, Tamiya N, Fromageot P (1976) Conformational changes in two neurotoxic proteins from snake venoms. Biochim Biophys Acta 453:121–132

Momany FA, McGuire RF, Burgess AW, Scheraga HA (1975) Energy parameters in polypeptides. VII. Geometric parameters, par-

tial atomic charges, nonbonded interactions, hydrogen bond interactions, and intrinsic torsional proteins for the naturally occurring amino acids. J Phys Chem 79:2361–2381

Moras D, Olsen KW, Sabesan MN, Buehner M, Ford GC, Rossmann MG (1975) Studies of asymmetry in the three-dimensional structure of lobster D-glyceraldehyde-3-phosphate dehydrogenase. J Biol Chem 250:9137–9162

Morgan WT, Smith A (1984) Domain structure of rabbit hemopexin. Isolation and characterization of a heme-binding glycopeptide. J Biol Chem 259:12001–12006

Murrell JN, Harget AJ (1972) Semi-empirical molecular orbital theory of molecules. Wiley, London

Nishimoto K, Forster LS (1965) SCF calculations of aromatic hydrocarbons. The variable β approximation. Theor Chim Acta (Berlin) 3:407–417

Nishimoto K, Forster LS (1966) SCFMO calculations of heteroatomic systems with the variable β approximation. I. Heteroatomic molecules containing nitrogen or oxygen atoms. Theor Chim Acta (Berlin) 4:155–165

Ohmori D (1984) Characterization and reconstitution of *Pseudomonas ovalis* ferredoxin. Biochim Biophys Acta 790:15–21

Ooi T, Scott RA, Vanderkooi G, Scheraga HA (1967) Conformational analysis of macromolecules. IV. Helical structures of poly-L-alanine, poly-L-valine, poly-β-methyl-L-aspartate, poly-γ-methyl-L-glutamate, and poly-L-tyrosine. J Chem Phys 46:4410–4426

Österlund E, Eronen I, Österlund K, Vuento M (1985) Secondary structure of human plasma fibronectin: Conformational change induced by calf alveolar heparan sulfates. Biochemistry 24:2661–2667

Peggion E, Cosani A, Verdini AS, Del Pra A, Mammi M (1968) Conformational studies on poly-L-tryptophan: Circular dichroism and X-ray diffraction studies. Biopolymers 6:1477–1486

Perczel A, Hollósi M, Tusnády G, Fasman GD (1991) Convex constraints analysis: A natural deconvolution of circular dichroism curves of proteins. Prot Eng 4:669–679

Perczel A, Park K, Fasman GD (1992) Deconvolution of the circular dichroism spectra of proteins: The circular dichroism spectra of the antiparallel β-sheet in proteins. Proteins: Struct Funct Genet 13:57–69

Philips LA, Levy DH (1986a) The rotationally resolved electronic spectrum of indole in the gas phase. J Chem Phys 85:1327–1332

Philips LA, Levy DH (1986b) Determination of the transition moment and the geometry of tryptamine by rotationally resolved electronic spectroscopy. J Phys Chem 90:4921–4923

Platt JR (1949) Classification of spectra of cata-condensed hydrocarbons. J Chem Phys 17:484–495

Ponder JW, Richards FM (1987) Tertiary templates for proteins. Use of packing criteria in the enumeration of allowed sequences for different structural classes. J Mol Biol 193:775–791

Ponnuswamy PK, Sasisekharan V (1971) Studies on the conformation of amino acids. V. Conformation of amino acids with δ-atoms. Int J Protein Res 3:9–18

Przysiecki CT, Meyer TE, Cusanovich MA (1985) Circular dichroism and redox properties of high redox potential ferredoxins. Biochemistry 24:2542–2549

Richardson JS, Getzoff ED, Richardson DC (1978) The β-bulge: A common small unit of nonrepetitive protein structure. Proc Natl Acad Sci, USA 75:2574–2578

Ridley J, Zerner M (1973) An intermediate neglect of differential overlap technique for spectroscopy: pyrrole and the azines. Theor Chim Acta (Berlin) 32:111–134

Rodríguez-Romero A, Arreguín B, Hernández-Arana A (1989) Unusual far-ultraviolet circular dichroism of wheat germ agglutinin and hevein originated from cystine residues. Biochim Biophys Acta 998:21–24

Sasisekharan V, Ponnuswamy PK (1971) Studies on the conformation of amino acids. X. Conformations of norvalyl, leucyl and aromatic side groups in a dipeptide unit. Biopolymers 10:583–592

Sawyer L, Shotton DM, Campbell JW, Wendell PL, Muirhead H, Watson HC, Diamond R, Ladner RC (1978) The atom structure of crystalline porcine pancreatic elastase at 2.5 Å resolution. Comparison with the structure of α-chymotrypsin. J Mol Biol 118:137–208

Schellman JA (1968) Symmetry rules for optical rotation. Acc Chem Res 1:144–151

Sears DW, Beychok S (1973) Circular dichroism, in: Leach SJ (ed) Physical principles and techniques of protein chemistry, Part C. Academic Press, New York, pp 445–593

Shiraki M (1969) Circular dichroism and optical rotatory dispersion of N-acetylaromatic amino acid amides as models for proteins. Sci Pap Coll Educ Univ Tokyo 19:151–173

Siano DB, Metzler DE (1969) Band shapes of the electronic spectra of complex molecules. J Chem Phys 51:1856–1861

Smith WW, Burnett RM, Darling GD, Ludwig ML (1977) Structure of the semiquinone form of flavodoxin from *Clostridium MP.* Extension of 1.8 Å resolution and some comparisons with the oxidized state. J Mol Biol 117:195–225

Sreerama N, Woody RW (1993) A self-consistent method for the analysis of protein secondary structure from circular dichroism. Anal Biochem 209:32–44

Strickland EH (1974) Aromatic contributions to circular dichroism spectra of proteins. CRC Crit Rev Biochem 2:113–175

Takano T, Dickerson RE (1980) Redox conformation changes in refined tuna cytochrome c. Proc Natl Acad Sci, USA 77:6371–6375

Timasheff SN, Bernardi G (1970) Studies on acid deoxyribonuclease: VII. Conformation of three nucleases in solution. Arch Biochem Biophys 141:53–58

Tinoco I, Jr (1962) Theoretical aspects of optical activity. Part two: Polymers Adv Chem Phys 4:113–160

van Stokkum IHM, Spoelder HJW, Bloemendal M, van Grondelle R, Groen FCA (1990) Estimation of protein secondary structure and error analysis from circular dichroism spectra. Anal Biochem 191:110–118

Vuilleumier S, Sancho J, Loawenthal R, Fersht AR (1993) Circular dichroism studies of barnase and its mutants: Characterization of the contribution of aromatic side chains. Biochemistry 32:10303–10313

Watenpaugh KD, Sieker LC, Jensen LH (1980) Crystallographic refinement of rubredoxin at 1.2 Å resolution. J Mol Biol 138:615–633

Watson HC (1969) The stereochemistry of the protein myoglobin. Progr Stereochem 4:299–333

Wawrzynczak EJ, Drake AF, Thorpe PE (1988) Circular dichroism of isolated ricin A- and B-chains. Biophys Chem 31:301–305

Weigang OE, Jr (1966) Vibrational structuring in optical activity. Dev Appl Spectrosc 5:259–281

Woody RW (1968) Improved calculation of the $n\pi^*$ rotational strength in polypeptides. J Chem Phys 49:4797–4806

Woody RW (1978) Aromatic side-chain contributions to the far-ultraviolet circular dichroism of peptides and proteins. Biopolymers 17:1451–1467

Woody RW (1994) Circular dichroism. Methods Ezymol (in press)

Yamamoto Y, Tanaka J (1972) Polarized absorption spectra of crystals of indole and its related compounds. Bull Chem Soc Jpn 45:1362–1366

Yang CC, Chang CC, Hayashi K, Suzuki T, Ikeda K, Hamaguchi K (1968) Optical rotatory dispersion and circular dichroism of cobrotoxin. Biochim Biophys Acta 168:373–376

Yang JT, Wu C-SC, Martinez HM (1986) Calculation of protein conformation from circular dichroism. Methods Enzymol 130:208–269